



## VHE gamma-ray observations of the young synchrotron-dominated SNRs G1.9+0.3 and G330.2+1.0 with H.E.S.S.

IURI SUSHCH<sup>1,2</sup>✉, RYAN C. G. CHAVES<sup>3</sup>, MANUEL PAZ ARRIBAS<sup>1,4</sup>, FRANCESCA VOLPE<sup>3</sup>, NUKRI KOMIN<sup>5</sup>, MATTHIAS KERSCHHAGGL<sup>6</sup> FOR THE H.E.S.S. COLLABORATION

<sup>1</sup>*Humboldt University of Berlin, Germany*

<sup>2</sup>*Taras Shevchenko National University of Kyiv, Ukraine*

<sup>3</sup>*Max Planck Institute for Nuclear Physics, Heidelberg, Germany*

<sup>4</sup>*DESY, D-15735 Zeuthen, Germany*

<sup>5</sup>*LAPP, CNRS/IN2P3, Annecy-le-Vieux, France*

<sup>6</sup>*University of Bonn, Germany*

✉ [yusushch@physik.hu-berlin.de](mailto:yusushch@physik.hu-berlin.de)

**Abstract:** Supernova remnants (SNRs) are widely considered to be accelerators of cosmic rays (CR). They are also expected to produce very-high-energy (VHE;  $E > 100$  GeV) gamma rays through interactions of high-energy particles with the surrounding medium and photon fields. They are, therefore, promising targets for observations with ground-based imaging atmospheric Cherenkov telescopes like the H.E.S.S. telescope array. VHE gamma-ray emission has already been discovered from a number of SNRs, establishing them as a prominent source class in the VHE domain. Of particular interest are the handful of SNRs whose X-ray spectra are dominated by non-thermal synchrotron emission, such as the VHE gamma-ray emitters RX J0852.0-4622 (Vela Jr.) and RX J1713-3946. The shell-type SNRs G1.9+0.3 and G330.2+1.0 also belong to this subclass and are further notable for their young ages ( $\leq 1$  kyr), especially G1.9+0.3, which was recently determined to be the youngest SNR in the Galaxy ( $\sim 100$  yr). These unique characteristics motivated investigations with H.E.S.S. to search for VHE gamma rays. The results of the H.E.S.S. observations and analyses are presented, along with implications for potential particle acceleration scenarios.

**Keywords:** H.E.S.S. – SNR – G1.9+0.3 – G330.2+1.0

## 1 Introduction

Supernova remnants (SNRs) are believed to be sites of efficient particle acceleration and are expected to produce very-high-energy (VHE;  $E > 0.1$  TeV)  $\gamma$ -rays through the interaction of these accelerated, high-energy particles with ambient media and fields. VHE  $\gamma$ -ray emission is currently detected from a number of SNRs. Of particular interest are those SNRs whose X-ray spectra are dominated by non-thermal emission such as RX J0852.0–4622 (Vela Jr.) [1] and RX J1713–3946 [2]. Synchrotron emission from these SNRs reveals the existence of high-energy electrons implying strong particle acceleration at shock fronts of remnants. High-energy particles accelerated at shock fronts can produce VHE  $\gamma$ -rays through the inverse Compton (IC) scattering of relativistic electrons on ambient photon fields and/or through proton-proton interactions.

In this paper the results of the H.E.S.S. observations of two other SNRs with predominantly non-thermal X-ray emission, SNR G1.9+0.3 [3] and SNR G330.2+1.0 [4], are presented.

## 2 SNRs G1.9+0.3 and G330.2+1.0

### 2.1 G1.9+0.3

G1.9+0.3 is the youngest known Galactic supernova remnant. An age of about 100 years was derived from the expansion rate of the object obtained from the comparison of radio observations in 1985 and Chandra observations in 2007 [3]. This result was confirmed by independent radio observations [5, 6].

G1.9+0.3 was first identified as an SNR in a radio survey using the Very Large Array (VLA) at 4.9 GHz based on its shell-like morphology and non-thermal radio emission [7]. G1.9+0.3 had the smallest angular extent ever measured for a Galactic SNR ( $\sim 1.2'$ ).

Chandra observations 22 years later showed a significant expansion of the remnant to  $1.7'$  in diameter (about 16%) [3]. The X-ray image shows a nearly circular bright ring with extensions (“ears”) extruding symmetrically from the east and west sides. There is a significant difference in radio and X-ray morphologies: while the radio source has a brightness maximum to the north, the X-ray image reveals

a bilateral east-west symmetry. Observations revealed a featureless synchrotron-dominated X-ray spectrum [3] indicating the presence of a high-energy electron population. In the framework of the `srcut` model, which describes the synchrotron radiation from the exponentially cut-off power-law electron distribution, the roll-off frequency  $\nu_{\text{roll}} = 1.4 \times 10^{18}$  Hz (one of the highest values ever reported for SNRs) and the radio spectral index  $\alpha = 0.65$  were obtained. The very high column density of  $N_{\text{H}} = 5.5 \times 10^{22}$  cm $^{-2}$  suggests a distance of about 8.5 kpc. At this distance, the observed angular radius of the bright X-ray ring corresponds to  $\sim 2$  pc, or 2.2 pc including the “ears”. The observed expansion of the remnant leads to an estimate of the shock speed of 14000 km/s. For a sphere of radius 2.2 pc an explosion model with an exponential ejecta profile [8] predicts an age of 100 years and an ISM number density of about 0.04 cm $^{-3}$ . Slightly different values of the age, 80 years, and a number density of 0.018 cm $^{-3}$  are derived in [9], assuming an expansion velocity of 14000 km/s and a radius of 2 pc.

## 2.2 G330.2+1.0

The radio source G330.2+1.0 was identified as a Galactic SNR in [10] and [11] on the basis of its non-thermal spectrum and its proximity to the galactic plane. Subsequent observations at radio frequencies [12] showed the shell-like structure of the remnant with a gradient of surface brightness towards the galactic plane. G330.2+1.0 was classified as a possible composite type SNR in [13]. The angular diameter of the shell is  $\sim 11'$  [12, 13].

Based on ASCA observations [14], a featureless X-ray spectrum with a photon index of  $\Gamma \simeq 2.8$  and interstellar column density  $N_{\text{H}} \simeq 2.6 \times 10^{22}$  cm $^{-2}$  was discovered [4]. The X-ray spectrum was also fit with the `srcut` model deriving a roll-off frequency  $\nu_{\text{roll}} = 4.3 \times 10^{15}$  Hz and an absorption column density  $N_{\text{H}} \simeq 5.1 \times 10^{22}$  cm $^{-2}$  for the assumed radio spectral index  $\alpha = 0.3$ . X-ray observations revealed a general anticorrelation between radio and X-ray intensities.

Subsequent Chandra and XMM-Newton observations [15, 16] revealed that the X-ray emission from SNR G330.2+1.0 is dominated by a power-law continuum ( $\Gamma \sim 2.1 - 2.5$ ) and comes primarily from thin filaments along the boundary shell. A point-like source CXOU J160103.1-513353 was discovered with Chandra [15] at the center of the SNR, a possible central compact object (CCO). Chandra and XMM-Newton observations also revealed a faint thermal X-ray emission from G330.2+1.0 [16]. Using the thermal emission, a low ISM density of 0.1 cm $^{-3}$  was calculated. A lower limit on the distance  $d_{\text{G330}} \geq 4.9$  kpc was calculated in [17] using the HI absorption measurement. Hereafter, the distance to G330.2+1.0 is assumed to be 5 kpc. Obtained values of the ISM density and distance lead to the age estimate for the remnant of  $t_{\text{G330}} \simeq 1000$  years, using the Sedov

solution [18] to describe the hydro-dynamical expansion of the SNR at the adiabatic stage [16].

## 3 Observations and Analysis

### 3.1 The H.E.S.S. Instrument

H.E.S.S. (High Energy Stereoscopic System) is an array of four 13 m diameter imaging atmospheric Cherenkov telescopes (IACTs) located in the Khomas Highland of Namibia at an altitude of 1800 m above sea level [19, 20]. The telescopes are optimized for detection of very high energy  $\gamma$ -rays in the range of 100 GeV to 20 TeV by imaging Cherenkov light emitted by charged particles in an Extensive Air Shower (EAS). The total field of view of H.E.S.S. is  $5^\circ$  in diameter. The angular resolution of the system is  $\lesssim 0.1^\circ$  and the average energy resolution is about 15% [21]. The H.E.S.S. array is capable to detect point sources with a flux of 1% of the Crab Nebula flux at the significance level of  $5\sigma$  in 25 hours at low zenith angles [21].

### 3.2 Data Set and Analysis Results

For the study of G1.9+0.3 and G330.2+1.0, data taken in the period from 2004 to 2010 were compiled. SNR G1.9+0.3 is located  $\sim 2^\circ$  from the supermassive black hole Sgr A\* at the Galactic Center (GC). More than a half of the observations used for the analysis are therefore obtained from Sgr A\* observations. In order to reduce the high exposure gradient towards the GC, only those observations with a pointing within  $2.0^\circ$  from G1.9+0.3 were selected for the analysis. For SNR G330.2+1.0 all pointings within  $2.5^\circ$  from the center of the remnant were considered. After the standard H.E.S.S. quality selection [21] this resulted in 75 and 20 hours of livetime for G1.9+0.3 and G330.2+1.0, respectively (see Table 1).

The H.E.S.S. standard Hillas reconstruction [22] with standard cuts and the Reflected Region Background method [23] were used for the data analysis. The results were cross-checked using the alternative `Model analysis` technique [24] as well as independent calibration of the raw data and quality selection criteria.

No significant  $\gamma$ -ray signal was detected from G1.9+0.3 or G330.2+1.0. The 99% confidence level upper limits [25] on the integrated fluxes above 260 GeV (G1.9+0.3) and 380 GeV (G330.2+1.0) energy thresholds were calculated for three different assumed spectral indices, 2.0, 2.5 and 3.0 (see Table 2). The assumed spectral index does not have a major impact in the upper limits (see Fig. 1).

## 4 Discussion

VHE  $\gamma$ -rays from SNRs can be produced either via inverse Compton (IC) scattering of relativistic electrons on photon

Table 1: H.E.S.S. observations of SNRs G1.9+0.3 and G330.2+1.0

SNR	Observation period	Livetime	Mean offset angle	Mean zenith angle	Threshold energy
G1.9+0.3	2004–2010	75 h	1.5°	19°	0.26 TeV
G330.2+1.0	2004–2010	20 h	1.3°	32°	0.38 TeV

Table 2: Upper limits on the TeV  $\gamma$ -ray flux from SNRs G1.9+0.3 and G330.2+1.0

Spectral index	$F_{G1.9+0.3}(E > 260 \text{ GeV})$ , [ $\text{cm}^{-2} \text{s}^{-1}$ ]	$F_{G330.2+1.0}(E > 380 \text{ GeV})$ , [ $\text{cm}^{-2} \text{s}^{-1}$ ]
2.0	$< 3.8 \times 10^{-13}$	$< 1.4 \times 10^{-12}$
2.5	$< 4.6 \times 10^{-13}$	$< 1.6 \times 10^{-12}$
3.0	$< 5.3 \times 10^{-13}$	$< 1.8 \times 10^{-12}$

fields or via proton-proton interactions. In this paper the first scenario is discussed.

The radio and X-ray data were fit with the model of the synchrotron emission of an electron population with an energy distribution which follows a power-law with an exponential cut-off

$$\frac{dN_e}{dE} \propto E^{-p} e^{-E/E_{\text{cut}}}. \quad (1)$$

The distribution of relativistic electrons can be completely described by the set of three parameters: the spectral index  $p$ , the cut-off energy  $E_{\text{cut}}$  and the total energy in electrons  $W_{\text{tot}}$ . These parameters can be determined from the fit of the radio and X-ray data if the magnetic field  $B$  is known. Independently of the magnetic field, the fit of the synchrotron emission spectrum to radio and X-ray data can be defined by the similar set of three parameters: spectral index  $\alpha$ , roll-off energy  $E_{\text{roll}}$  and the spectrum normalization at 1 GHz. The electron spectral index  $p$  is directly connected to  $\alpha$  through the expression  $p = 2\alpha + 1$ , while  $E_{\text{cut}}$  and  $W_{\text{tot}}$  together with the synchrotron spectrum parameters depend also on the magnetic field.

Assuming different values for the magnetic field, the gamma-ray emission created by the same population of electrons via IC scattering on ambient photon fields (infrared (IR) and CMB) is predicted (Fig 2). The photon distribution is derived from the interstellar radiation field (ISRF) model [26] and is fit with three Planck distributions of optical, IR and CMB photons. The contribution of the optical photons to the  $\gamma$ -ray flux is found to be negligible. The upper limit on the TeV flux leads to an estimate of a lower limit of the magnetic field. This in turn allows to determine upper limits on the electron cut-off energy and the total energy in electrons (see Table 3).

Recently, the first synchrotron-dominated SNR RX J1713.7-3946 was discovered in GeV  $\gamma$ -rays [27]. The observed spectrum favours the leptonic model and implies a

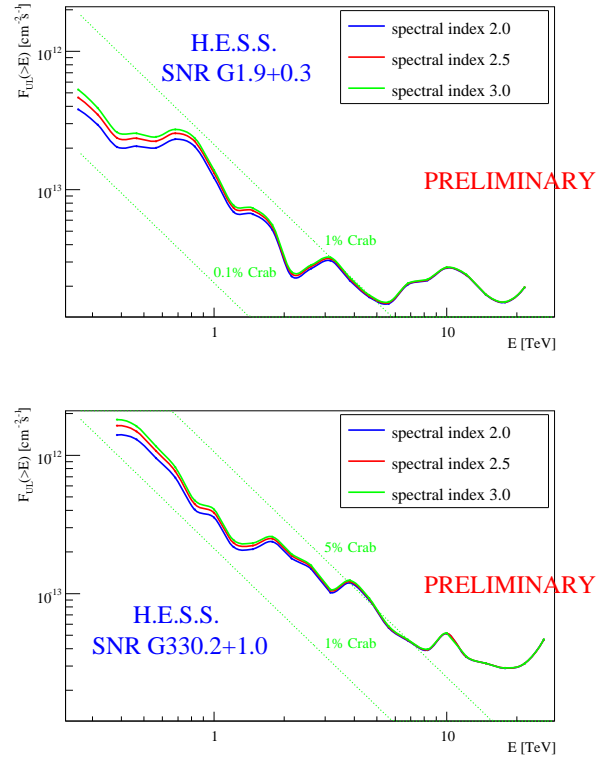


Figure 1: The upper limit (99% confidence level) of the integrated TeV  $\gamma$ -ray flux from SNRs G1.9+0.3 (top) and G330.2+1.0 (bottom) for three different assumed spectral indices,  $\Gamma = 2.0, 2.5$  and  $3.0$ .

very low magnetic field of  $\simeq 10 \mu\text{G}$  which is comparable to the limits found for G1.9+0.3 and G330.2+1.0.

## 5 Summary

Results from H.E.S.S. observations of two SNRs with dominantly non-thermal X-ray spectra, G1.9+0.3 and G330.2+1.0, were presented. 99% confidence level upper limits on the TeV flux from these sources were estimated. For an assumed spectral index of 2.5, the upper limits are found to be  $F_{G1.9}(> 260 \text{ GeV}) < 4.6 \times 10^{-13} \text{ cm}^{-2} \text{s}^{-1}$  for G1.9+0.3 and  $F_{G330}(> 380 \text{ GeV}) < 1.6 \times 10^{-12} \text{ cm}^{-2} \text{s}^{-1}$  for G330.2+1.0.

Upper limits on the VHE flux allow to derive constraints on the interior magnetic field in the framework of a lep-

Table 3: SED model fitting parameters

SNR	G1.9+0.3	G330.2+1.0
$p$	2.2	2.2
$E_{\text{roll}}$ , [KeV]	2.0	0.2
$B$ , [ $\mu\text{G}$ ]	$> 15$	$> 14$
$E_{\text{cut}}$ , [TeV]	$< 50$	$< 17$
$W_{\text{tot}}$ , [erg]	$< 3.1 \times 10^{48}$	$< 5.7 \times 10^{48}$

tonic emission scenario. The obtained lower limits on the magnetic fields are comparable to the estimates of magnetic fields in SNRs in which VHE emission can be explained by an IC mechanism.

G330.2+1.0 and G1.9+0.3 remain promising targets for observations at VHE and could be detectable with future, more sensitive instruments like the Cherenkov Telescope Array (CTA).

## References

- [1] F. Aharonian *et al.*, *ApJ*, 2007, **661**: 236–249
- [2] F. Aharonian *et al.*, *A&A*, 2007, **464**: 235–243
- [3] S. P. Reynolds *et al.*, *ApJ*, 2008, **680**: L41–L44
- [4] K. Torii *et al.*, *PASJ*, 2006, **58**: L11–L14
- [5] D. A. Green *et al.*, *MNRAS*, 2008, **387**: L54–L58
- [6] T. Murphy, B. M. Gaensler, S. Chatterjee, *MNRAS*, 2008, **389**: L23–L27
- [7] D. A. Green, S. F. Gull, *Nature*, 1984, **312**: 527–529
- [8] V. V. Dwarkadas, R. A. Chevalier, *ApJ*, 1998, **497**: 807
- [9] L. T. Ksenofontov, H. J. Völk, E. G. Berezhko, *ApJ*, 2010, **714**: 1187–1193
- [10] D. H. Clark, J. L. Caswell, A. J. Green, *Nature*, 1973, **246**: 27–30
- [11] D. H. Clark, J. L. Caswell, A. J. Green, *Aust. J. Phys. Astrophys. Suppl.*, 1975, **37**: 1–38
- [12] J. L. Caswell *et al.*, *MNRAS*, 1983, **204**: 915–920
- [13] J. B. Z. Whiteoak, A. J. Green, *A&AS*, 1996, **118**: 329–380
- [14] Y. Tanaka, H. Inoue, S.S. Holt, *PASJ*, 1994, **46**: L37
- [15] S. Park *et al.*, *ApJ*, 2006, **653**: L37–L40
- [16] S. Park *et al.*, *ApJ*, 2009, **695**: 431–441
- [17] N. M. McClure-Griffiths *et al.*, *ApJ*, 2001, **551**: 394–412
- [18] L. I. Sedov: 1959, *Similarity and Dimensional Methods in Mechanics*, Academic Press, New York
- [19] K. Bernloehr *et al.*, *Astropart. Phys.*, 2003, **20**: 111
- [20] S. Funk *et al.*, *Astropart. Phys.*, 2004, **22**: 285
- [21] F. Aharonian *et al.*, *A&A*, 2006, **457**: 899–917
- [22] Aharonian, F., Akhperjanian, A. G., Bazer-Bachi, A. R., *et al.* 2006, *A&A*, 457, 899
- [23] Berge, D., Funk, S., & Hinton, J. 2007, *A&A*, 466, 1219
- [24] M. de Naurois, L. Rolland, *Astropart. Phys.*, 2009, **32**: 231–252
- [25] Feldman, G. J. & Cousins, R. D. 1998, *PHYS.REV.D*, 57, 3873
- [26] Porter, T. A., Moskalenko, I. V., & Strong, A. W. 2006, *ApJ*, 648, L29
- [27] Abdo, A. A., *et al.* 2011, *ApJ*, 734, 28

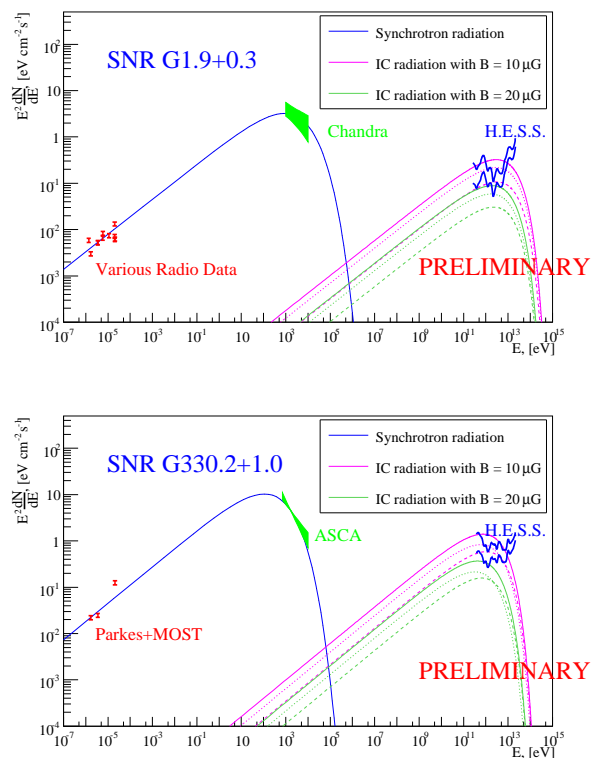


Figure 2: Spectral energy distribution (SED) of the broadband emission from the SNRs G1.9+0.3 and G330.2+1.0. The H.E.S.S. upper limits are shown assuming two different spectral indices: 2.0 (lower curve) and 3.0 (upper curve). The various radio data for G1.9+0.3 were compiled in [5]. For the IC emission: dashed lines correspond to the IC on IR photons, dotted lines to the IC on CMB photons, solid lines to the total IC emission